Functional Polyacetylenes: Synthesis, Thermal Stability, Liquid Crystallinity, and Light Emission of Polypropiolates

Jacky W. Y. Lam, Jingdong Luo, Yuping Dong, Kevin K. L. Cheuk, and Ben Zhong Tang*

Department of Chemistry, Center for Display Research, Institute of Nano Science and Technology, and Open Laboratory of Chirotechnology of the Institute of Molecular Technology for Drug Discovery and Synthesis,† Hong Kong University of Science & Technology, Clear Water Bay, Kowloon, Hong Kong, China

Received June 27, 2002; Revised Manuscript Received September 4, 2002

ABSTRACT: Polypropiolates with different kinds and numbers of substituents (−{(R)C═C[$CO_2(CH_2)_6$−OCO−Biph−OC_7H_{15}]}$_n$−; R = H (**1**), CH_3 (**2**), C_6H_5 (**3**), Biph = 4,4′-biphenylyl) were synthesized, and the effects of the structural variations on the mesomorphic and luminescent properties of the polymers were investigated. The propiolate monomers RC≡$CCO_2(CH_2)_6$OCO−Biph−OC_7H_{15} [R = H (**8**), CH_3 (**9**), C_6H_5 (**10**)] were prepared by esterification of (substituted) propiolic acids (RC≡CCO_2H) in high yields. While **8** and **9** formed enantiotropic SmA phases, **10** was nonmesomorphic. Polymerizations of the monomers were effected by Mo- and Rh-based catalysts and polypropiolates with high molecular weights (M_w up to 3.5×10^5 Da) were obtained in moderate yields. The polymers were characterized by IR, NMR, TGA, DSC, POM, XRD, UV, and PL analyses. All the polymers were thermally stable. Polymer **1** obtained from the Mo catalyst possessed a lower stereoregularity but exhibited a better-packed monolayer SmA mesostructure, in comparison to the polymer from the Rh catalyst. With an increase in the backbone rigidity from **1** to **3**, the glass transition temperature of the chain segments increased, but packing order of the mesogen pendants decreased. Upon photoexcitation, all the polymers emitted UV light of 369 nm. The emission efficiency was dramatically affected by the chain stereoregularity and backbone structure, with **2** exhibiting a quantum yield as high as 0.7.

Introduction

The successful preparation of polyacetylene film and the discovery of metallic conductivity of its doped form have opened up a new research area, "plastic electronics".[1] Polyacetylene is, however, notoriously intractable and unstable, which has greatly detracted from its potential for technological applications. Attachments of aromatic pendants to the polyacetylene backbone have helped solve the intractability and degradation problems and have generated readily processable and thermally stable substituted polyacetylenes;[2,3] for example, poly(1-phenyl-1-alkyne)s are soluble in common solvents and do not decompose at elevated temperatures for a prolonged period of time.[3a] Incorporation of polar substituents to the polyacetylene structure will impart new functionalities to the conjugated polymer, but the early attempts in polymerizing functional acetylene derivatives via the metathesis route catalyzed by early transition-metal compounds such as $MoCl_5$ and WCl_6 have met with only limited success. For example, the polymerizations of alkynes with functionalities of alcohol,[4] acid,[5] ester,[6] ether,[7] thio,[7a] amine,[8] nitrile,[6a,9] and phosphonium[10] often gave oligomeric or insoluble products, normally in low yields.

In our recent pursuit of developing functional polyacetylenes with mesomorphic, luminescent, and photoconductive properties,[11−20] we have succeeded in polymerizing mono- and disubstituted acetylenes containing mesogenic and chromophoric groups with ester,[12] ether,[13] amine,[14] thio,[15] cyano,[16] vinyl,[17] and ethynyl[18] functionalities using molybdenum-, tungsten-, and niobium-based metathesis catalysts.[19,20] The functional pendants in all these polymers are, however, separated from the polyacetylene backbone by aliphatic spacers (**4**) or aryl rings (**5**; Chart 1). We are interested in directly attaching functional pendants to the polyacetylene backbone, and in this work, we extended our synthetic efforts to the polymerizations of substituted propiolates (RC≡CCO_2R′), in which the carbonyloxy group and the triple bond are located in immediate vicinity.

Chart 1

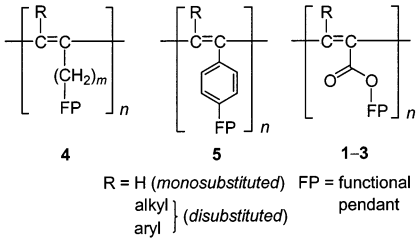

The carbonyloxy group will perturb the electronic states of the triple bond of the propiolates and also of the double-bond backbone of the polypropiolates—such electronic interactions are expected to affect chemical reactivity of the monomers and materials properties of the polymers. Indeed, polymerizability of propiolates seemed to be low,[5,6] due possibly to the electronic and steric effects of the carbonyl group. There have been only a few scattered reports over a large time span on the polymerizations of propiolates using $MoCl_5$- and WCl_6-based metathesis catalysts, with most of the attempts ended with failure.[2,5,6] Although HC≡CCO_2R can now be polymerized by insertion catalysts based on an expensive later transition metal of rhodium,[21] effective polymerizations of R′C≡CCO_2R (R′ ≠ H) have never

† An Area of Excellence Scheme administrated by the University Grants Committee of Hong Kong.

* Corresponding author: phone +852-2358-7375; Fax +852-2358-1594; e-mail tangbenz@ust.hk.

10.1021/ma021011a CCC: $22.00
Published on Web 09/28/2002

Table 1. Thermal Transitions and Corresponding Thermodynamic Parameters of Substituted Propiolate Monomers 8−10[a]

	T, °C [Δ*H*, kJ/mol; Δ*S*, J/(mol K)]	
monomer	cooling	heating
8	i 54.0 (−6.90; −21.10) SmA 40.0 (−34.2; −109.30) k	k 58.7 (−3.96; −11.94) k′ 66.2 (−) SmA 69.40 (52.05; 152.02)[b] i
9	i 40.3 (−7.33; −23.40)[b] SmA 33.5 (−) k	k 39.5 (−) SmA 44.0 (6.74; 21.26)[b] i
10	(amorphous solid)[c]	(amorphous solid)[c]

[a] Data taken from the DSC thermograms recorded under nitrogen during the first cooling and second heating scans. Abbreviations: k = crystalline state, Sm = smectic phase, i = isotropic liquid. [b] Sum of the overlapping transitions. [c] No any transition peaks were recorded.

Scheme 1

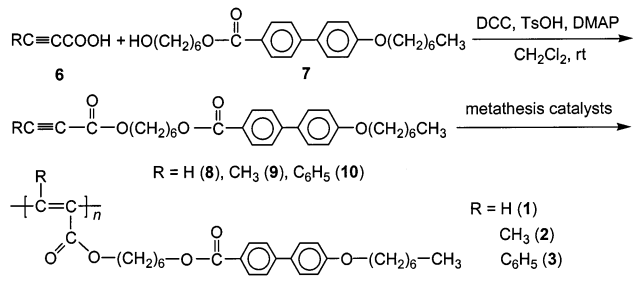

Table 2. Polymerization of 6-{[(4′-Heptyloxy-4-biphenylyl)carbonyl]oxy}hexylpropiolate (8)[a]

no.	catalyst[b]	solvent	temp (°C)[c]	yield (%)	M_w[d]	M_w/M_n[d]
1	$[Rh(nbd)Cl]_2$	CH_3CN	40	40.3	353 600	2.7
2	$[Rh(cod)Cl]_2$	CH_3CN	40	4.0	88 740	6.0
3	$Rh(cod)(NH_3)Cl$	CH_3CN	40	11.9	40 180	3.3
4	$Rh(nbd)(tos)(H_2O)$	CH_3CN	40	0		
5	$Rh(cod)(tos)(H_2O)$	CH_3CN	40	3.1	157 200	9.9
6	$MoOCl_4-Ph_4Sn$	toluene	60	36.9	16 280	1.6
7	$MoCl_5-Ph_4Sn$	toluene	rt	28.1	17 540	1.6
8	$MoCl_5-Ph_4Sn$	toluene	60	47.4	23 190	2.0
9	$MoCl_5-Ph_4Sn$	toluene	80	34.3	20 090	1.9
10	$WOCl_4-Ph_4Sn$	toluene	60	0		
11	WCl_6-Ph_4Sn	toluene	60	23.4	9 451	1.5

[a] Carried out under nitrogen for 24 h; $[M]_0 = 0.2$ M, [cat.] = [cocat.] = 10 mM; for Rh-based catalysts, [cat.] = 2 mM. [b] Abbreviations: nbd = 2,5-norborndiene, tos = *p*-toluenesulfonate. [c] rt = room temperature. [d] Determined by GPC in THF on the basis of a polystyrene calibration.

been realized by either insertion or metathesis catalysts.[2,21−23]

A variety of substituted propiolates can be readily derived by a simple esterification procedure from commercially available propiolic acids, and successful development of effective polymerization systems will offer a large palette for the design and synthesis of functional substituted polyacetylenes. To prove the feasibility and to demonstrate the versatility of this approach, in this work, we prepared a group of propiolates with mono- [R = H (**8**)] and disubstitutions [R = CH_3 (**9**), C_6H_5 (**10**)] and with biphenyl-based mesogenic and chromophoric functional groups (Scheme 1). We successfully polymerized, using inexpensive Mo-based metathesis catalysts, the new propiolates to high molecular weight polymers. We studied the materials properties of the new polymers and found that the propiolic carbonyloxy groups in the neighborhood of the main-chain double bonds electronically perturbed and sterically rigidified the polyene, which in turn altered the thermal stability, liquid crystallinity, and luminescence behaviors of the polypropiolates.

Results and Discussion

Synthesis and Mesomorphism of the Monomers. We prepared three biphenyl-containing propiolate monomers (**8**−**10**) by esterifications of 6-hydroxy-1-hexyl (4-heptyloxy-4′-biphenylyl)carboxylate (**7**)[24] with (substituted) propiolic acids (**6**) in the presence of 1,3-dicyclohexylcarbodiimine (DCC), *p*-toluenesulfonic acid (TsOH), and 4-(dimethylamino)pyridine (DMAP). The reactions went smoothly, and the products were isolated in high yields (≥76%) after purifications by silica gel chromatography followed by recrystallization.

All the monomers were white solids at room temperature. Monomers **8** and **9** showed mesomorphism at elevated temperatures. Upon cooling the isotropic liquids of the two monomers, typical focal−conic textures of SmA phase were observed. Reheating the monomers regenerated the textures, revealing the enantiotropic nature of the mesophase transformations. The thermal transitions and corresponding thermodynamic parameters of the monomers are summarized in Table 1. The phase transitions of **8** involved abnormally large enthalpy and entropy changes [Δ*H* up to ∼52 kJ/mol and Δ*S* up to ∼152 J/(mol K)], suggesting that liquid crystalline dimers may be acting as virtual mesogenic units.[12a,c,25] Two molecules of monomer **8** may form a dimer through hydrogen bonding between their acetylenic hydrogen and carbonyl oxygen. The packing of the bulky dimers may cause a big change in the order of the system, and the disassembling of the ordered dimers may involve cleavage of the hydrogen bonds; such packing and disassembling processes thus bring about the large Δ*S* and Δ*H* changes. When the acetylenic hydrogen is replaced by a methyl group in **9**, the Δ*H* and Δ*S* changes in its thermal transitions became smaller, due to the lack of intermolecular hydrogen bonding. When a phenyl ring is attached to the triple bond of propiolate, the situation became even worse: no thermal transition peaks were recorded during the first cooling and second heating scans in the DSC analysis of **10**, although its crystals obtained from the recrystallization process exhibited a melting peak in the first heating scan. This suggests that the packing process of the molecules of **10** is very slow—so slow that the sample remained amorphous without entering any ordered states in the time scale of the DSC measurements.

Polymerizations by Transition-Metal Catalysts. We tried to polymerize the propiolate monomers with transition-metal catalysts. Organorhodium complexes are known to effect insertion polymerizations of propiolic esters,[21] but we found that not all the Rh complexes could initiate the polymerization of propiolate **8**. While $[Rh(nbd)Cl]_2$ worked well (Table 2, no. 1; this polymer being denoted as "**1**-Rh" in our future discussions), the Rh complexes with other ligands all failed to give polymeric products in satisfactory yields. Disappointed by the Rh results, we turned our attention to metathesis catalysts and checked whether the functional propiolate could be polymerized with early-transition-metal initiators. We tested a mixture of $MoOCl_4$ and Ph_4Sn and

Table 3. Polymerization of 6-{[(4′-Heptyloxy-4-biphenylyl)carbonyl]oxy}hexyl-2-butynate (9)[a]

no.	catalyst[b]	solvent	temp (°C)[c]	yield (%)	M_w[d]	M_w/M_n[d]
1	$[Rh(nbd)Cl]_2$	CH_3CN	40	0		
2	$MoOCl_4-Ph_4Sn$	toluene	60	0		
3	$MoCl_5$	toluene	rt	31.2	6 861	1.5
4	$MoCl_5-Ph_4Sn$	toluene	rt	28.8	11 020	2.0
5	$MoCl_5-Ph_4Sn$	toluene	60	44.0	9 190	2.1
6	$MoCl_5-Ph_4Sn$	dioxane	rt	0		
7	$MoCl_5-Ph_4Sn$	dioxane	60	trace		
8	$Mo(nbd)(CO)_4$	CCl_4	60	9.9	41 640	3.2
9	WCl_6-Ph_4Sn	toluene	rt	trace		
10	WCl_6-PhSn	toluene	60	trace		
11	WCl_6-PhSn	dioxane	60	trace		
12	$WOCl_4-Ph_4Sn$	toluene	60	0		
13	$W(mes)(CO)_3$	CCl_4	60	trace		

[a] Carried out under nitrogen for 24 h; $[M]_0 = 0.2$ M, [cat.] = [cocat.] = 10 mM; for $[Rh(nbd)Cl]_2$, [cat.] = 0.2 mM. [b] Abbreviations: nbd = 2,5-norborndiene, mes = mesitylene. [c] rt = room temperature. [d] Determined by GPC in THF on the basis of a polystyrene calibration.

found that it polymerized **8** in a moderate yield. Although no any successful examples have been reported in the literature[2,22] in using $MoCl_5$ as catalyst for propiolate polymerizations, we found that **8** could be converted by $MoCl_5-Ph_4Sn$ to a high molecular weight polymer in a good yield (Table 2, no. 8; this polymer being denoted as "**1**-Mo" in our future discussions). The $WOCl_4-Ph_4Sn$ mixture failed to give any polymeric product, which is in some sense expected, because W compounds have been known to be noncatalysts for polymerizations of electron-deficient acetylenes with electron-withdrawing groups directly attached to the triple bonds (e.g., W compounds cannot initiate polymerizations of halogen-containing acetylenes such as 1-halo-1-alkynes and 1-halo-2-phenylacetylenes).[19,27] To our surprise, however, WCl_6-Ph_4Sn exhibited some catalytic activity for the polymerization of **8**, although both yield and molecular weight of the resultant polymer were low (Table 2, no. 11).

Encouraged by the good results of the Mo-catalyzed polymerizations of **8**, we went one step further and investigated the polymerizations of disubstituted propiolates **9** and **10**, which have never been polymerized by any catalyst systems. Table 3 summarizes the polymerization behaviors of **9**. This monomer, different from **8**, could not be polymerized by $[Rh(nbd)Cl]_2$ and $MoOCl_4$ (Table 3. nos. 1 and 2). Delightfully, however, the polymerizations catalyzed by $MoCl_5(-Ph_4Sn)$ in toluene gave polymeric products, whose yield increased with an increase in the polymerization temperature. Dioxane was a bad solvent: only a trace amount of polymer was produced even when the polymerization was carried out at a high temperature. The $Mo(nbd)(CO)_4$ complex is air- and moisture-stable and can polymerize a variety of functional acetylenes in both halogenated and nonhalogenated solvents.[19,28] This complex was also active in polymerizing **9** although the polymer yield was low (~10%). Irrespective of cocatalyst, solvent, and temperature, all the W catalysts failed to effectively initiate the polymerization of **9**.

Similarly, the organorhodium catalyst failed to polymerize **10** (Table 4, no. 1). Different from its methyl-substituted cousin (**9**), the phenyl-substituted propiolate (**10**) could be polymerized with $MoOCl_4-Ph_4Sn$, although the catalytic efficiency was low. $MoCl_5$ alone was ineffective in polymerizing **10**. Addition of Ph_4Sn co-

Table 4. Polymerization of 6-{[(4′-Heptyloxy-4-biphenylyl)carbonyl]oxy}hexylphenylpropiolate (10)[a]

no.	catalyst[b]	solvent	temp (°C)[c]	yield (%)	M_w[d]	M_w/M_n[d]
1	$[Rh(nbd)Cl]_2$	CH_3CN	40	0		
2	$MoOCl_4-Ph_4Sn$	toluene	60	6.5	133 100	3.6
3	$MoCl_5$	toluene	60	trace		
4	$MoCl_5-Ph_4Sn$	toluene	rt	51.0	196 400	2.7
5	$MoCl_5-Ph_4Sn$	toluene	60	56.8	239 300	3.2
6	$MoCl_5-Ph_4Sn$	toluene	80	56.8	119 800	3.5
7	$MoCl_5-Ph_4Sn$	dioxane	60	50.1	23 550	3.1
8	WCl_6-Ph_4Sn	toluene	rt	trace		

[a] Carried out under nitrogen for 24 h; $[M]_0 = 0.2$ M, [cat.] = [cocat.] = 10 mM; for $[Rh(nbd)Cl]_2$ catalyst, [cat.] = 0.2 mM. [b] Abbreviation: nbd = 2,5-norborndiene. [c] rt = room temperature. [d] Determined by GPC in THF on the basis of a polystyrene calibration.

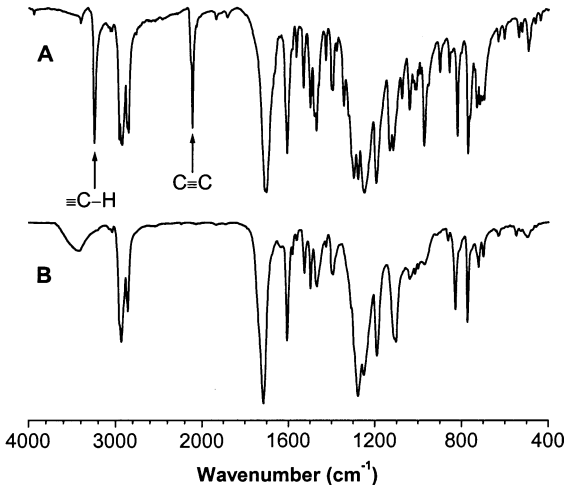

Figure 1. IR spectra of (A) monomer **8** and (B) its polymer **1** (sample from Table 2, no. 8).

catalyst, however, dramatically activated the Mo catalyst and greatly boosted the polymer yield. The yield was not sensitive to the changes in the temperature and solvent, and the polymerization proceeded well in dioxane. Like **9**, **10** again underwent sluggish polymerization in the presence of WCl_6-Ph_4Sn. It should be stressed here that the results for the polymerizations of **10** catalyzed by the $MoCl_5-Ph_4Sn$ mixture are truly remarkable. The organorhodium complexes have been heralded as effective catalysts for the insertion polymerizations of propiolates, but the polymer yields are normally in the range ~30−40%.[21] In addition, the catalysts are ineffective for polymerizations of disubstituted acetylenes. The Mo catalyst, however, effected the polymerization of the disubstituted acetylene **10**, giving high molecular weight polymers in high yields (>50%).

Structural Characterizations by Spectroscopies. The polymeric products were characterized by spectroscopic methods, and all the polymers gave satisfactory analysis data corresponding to their expected molecular structures (see Experimental Section for details). An example of the IR spectrum of polymer **1** is shown in Figure 1; the spectrum of its monomer **8** is also given for comparison. The monomer showed strong absorption bands at 3245 and 2113 cm^{-1}, due respectively to ≡C−H and C≡C stretching vibrations. The latter band is somewhat unexpected because almost no signals were observed at wavenumbers around 2113 cm^{-1} in the IR spectra of monosubstituted acetylenes of $HC{\equiv}C(CH_2)_m-OCO-Biph-OC_7H_{15}$[12c] and $HC{\equiv}CC_6H_4CO_2(CH_2)_6OCO-$

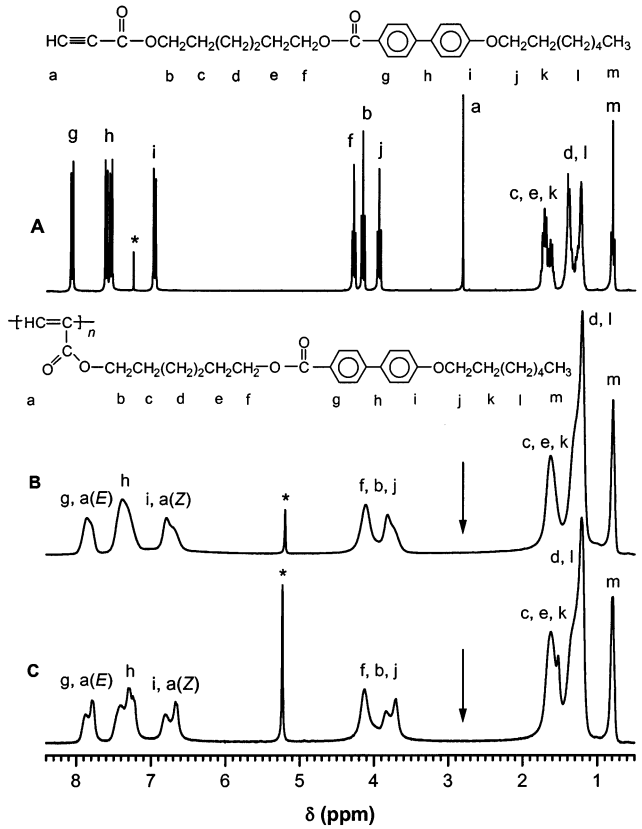

Figure 2. ^{1}H NMR spectra of (A) monomer **8** and its polymer prepared by (B) $MoCl_5-Ph_4Sn$ (**1**-Mo; sample from Table 2, no. 8) and (C) $[Rh(nbd)]_2$ catalysts (**1**-Rh; Table 2, no. 1). The resonance peaks of the solvents (chloroform for **8** and dichloromethane for **1**) are marked with * symbols.

Biph$-OC_7H_{15}$.[24] Comparing these acetylenes with **8** [$HC{\equiv}CCO_2(CH_2)_6OCO-Biph-OC_7H_{15}$], one can immediately recognize the major structural difference: **8** has a carbonyloxy group directly linked to the acetylene triple bond. The electronic communication between the CO_2 and C≡C groups is obviously responsible for the strong C≡C stretching band at 2113 cm^{-1}.[29] Both the ≡C−H and C≡C bands disappeared in the spectrum of polymer **1**, confirming that the acetylene triple bond has been completely consumed in the Mo-catalyzed metathesis polymerization. Similar to **1**, polymers **2** and **3** showed no triple-bond-related stretching vibrations in their IR spectra.

Figure 2 shows ^{1}H NMR spectra of monomer **8** and its polymers prepared with $MoCl_5-Ph_4Sn$ (**1**-Mo) and $[Rh(nbd)Cl]_2$ catalysts (**1**-Rh). The acetylene proton of the monomer exhibited a strong resonance peak at δ 2.88, which completely disappeared in the spectra of its polymers. The spectrum of **1**-Rh was better resolved than that of **1**-Mo, indicating that the polymer prepared from the Rh catalyst possesses better stereoregularity than that from the Mo catalyst, in agreement with the general observation that Rh-catalyzed acetylene polymerizations normally proceed in a stereoregular fashion.[21,22] To figure out the stereostructure of **1**-Rh, we closely inspected its aromatic and olefinic resonance peaks. There exist four theoretically possible stereostructures[30] for the chain segments of **1**, as shown in Chart 2. The *E-s-E* and *Z-s-Z* isomeric structures may have not been formed in the propiolate polymerization due to obvious steric reasons,[2,22] which thus can be excluded from our discussions. Calculations based on Shoolery's rules[31] suggest that the *E-s-Z* and *Z-s-E*

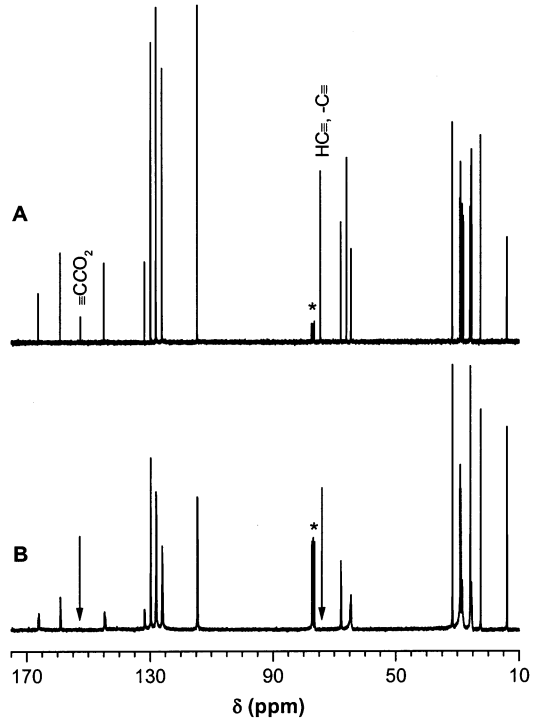

Figure 3. ^{13}C NMR spectra of (A) monomer **8** and (B) its polymer **1** (sample from Table 2, no. 8). The resonance peaks of chloroform solvent are marked with * symbols.

Chart 2

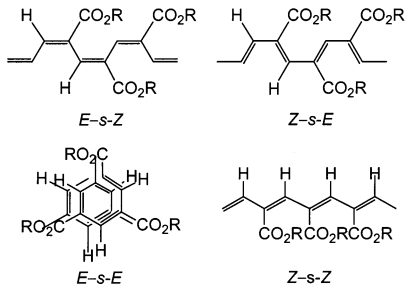

isomers resonate at δ 7.65 and 6.75, respectively. Several groups have reported that their polypropiolates prepared by the Rh catalysts absorbed at δ ~7.7,[21e] ~6.8,[21d] and 6.57.[21b] The peaks at δ 7.83 and 6.74 in the spectrum of **1**-Rh (Figure 2C) thus may be assigned to the absorptions by the olefinic protons of the *E-s-Z* and *Z-s-E* isomers, respectively, although their overlapping with the absorption peaks of the aromatic protons hampered quantitative estimation of its *E*/*Z* contents. The complete merge of the olefinic and aromatic peaks of the stereoirregular polymer **1**-Mo, on the other hand, prohibited us from making any meaningful discussions on its stereostructures.

Figure 3 shows the ^{13}C NMR spectrum of polymer **1** along with that of its monomer **8**. While the acetylenic carbon atoms of **8** resonated at δ 74.60 and 74.57, these peaks were absent in the spectrum of **1**. The transformation of the acetylene triple bond to the polyene double bond by the acetylene polymerization downfield-shifted the absorption peak of the carbonyl carbon directly linked to the triple bond (≡C*C*O_2) from δ 152.6 to 166.0,[21f] which overlapped with the peak of the carbonyl carbon linked to the biphenyl ring (O*C*O−Biph) in the spectrum of the polymer. It has been reported that the absorption peaks of the olefinic carbon atoms of poly(methyl propiolate) resonate at δ 134 and 128.[21f] Be-

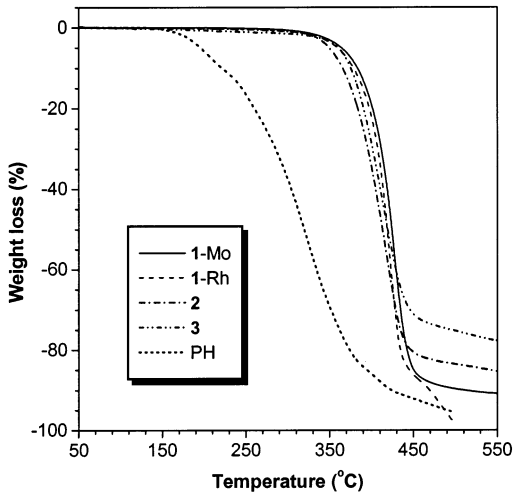

Figure 4. TGA thermograms of **1**-Mo (sample from Table 2, no. 8), **1**-Rh (Table 2, no. 1), **2** (Table 3, no. 5), and **3** (Table 4, no. 5) recorded under nitrogen at a heating rate of 10 °C/min. The thermogram of poly(1-hexyne) (PH) is shown for comparison (data taken from ref 3a).

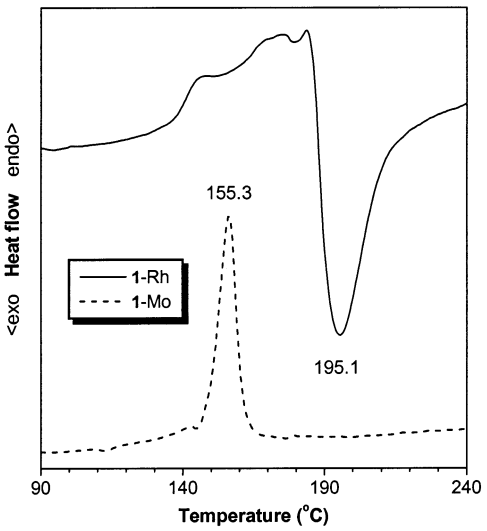

Figure 5. DSC thermograms of **1**-Rh (sample from Table 2, no. 1) and **1**-Mo (Table 2, no. 8) recorded under nitrogen during the first heating scan at a scan rate of 10 °C/min.

cause of the structural similarity, **1** may absorb in the same spectral region at δ 131.7 (=CCO_2) and 128.0 (=CH), which, however, overlap with the resonance peaks of its aromatic protons. Although **1**-Rh exhibited better-structured ^{1}H NMR spectrum than **1**-Mo, no such difference was observed in their ^{13}C spectra.

Thermal Stability and Isomerization. Monosubstituted polyacetylenes such as poly(1-alkynes) of general structure $-\{HC{=}C[(CH_2)_mCH_3]\}_n-$ are thermally unstable: for example, poly(1-hexyne) (PH) starts to lose its weight at ~150 °C.[3a] Polypropiolate **1** $-\{HC{=}C[CO_2{-}(CH_2)_mCH_2R)]\}_n-$ is in some sense a structural congener of poly(1-alkyne) with a carbonyloxy (CO_2) group inserted between a polyene double bond and an alkyl pendant. Unlike PH, **1** exhibited a weight loss temperature as high as ~350 °C (Figure 4). This enhanced thermal stability is probably due, at least in part, to the electron-withdrawing carbonyloxy group, which may have reduced the reactivity of the polymer through its electronic interactions with the polyene backbone. The stability of the polypropiolates changed little with the preparation method (Mo or Rh catalyst) and the pendant number (mono- or disubstitution): all polymers **1**−**3** lost almost no weights below ~350 °C.

The better-defined ^{1}H NMR spectrum of **1**-Rh suggests that the polymer possesses a long persistence length of stereoregular chain segments (cf. Figure 2C). We thus checked whether **1**-Rh would undergo thermally induced isomerization. When the polymer was heated (first heating scan), it exhibited a broad endothermic hump in the temperature region of ~125−185 °C, followed by a deep exothermic valley at ~195 °C (Figure 5). Polarized optical microscope (POM) observation revealed that the former was partly associated with isotropization (vide infra), and NMR analysis suggested that the latter was partially related to isomerization.[24] The endothermic isomerization process commenced before the exothermic isotropization transition finished, which hindered the hump from developing into a defined peak. Upon isomerization, the NMR peaks of the polymer became broadened, which frustrated our effort to decipher the involved mechanism. Unlike stereoregular **1**-Rh, its stereoirregular cousin **1**-Mo gave only one peak associated with isotropization but not isomerization. The lack of the latter process allowed the former transition to develop into a sharp peak in the DSC thermogram. The NMR spectrum of **1**-Mo changed little upon the thermal treatment, which further verifies the stereoirregular nature of its chain segments.

Mesomorphic Transition and Mesogenic Packing. The electronic and steric effects of the propiolic carbonyloxy group may rigidify the polypropiolate backbone. When the propiolic β-hydrogen is further replaced by another substituent, the steric crowdedness in the constitutional repeat unit of the resultant disubstituted polypropiolates may make the polyacetylene backbone even stiffer.[3b,c] A rigid polymer backbone often distorts the packing arrangement of mesogenic pendants in a side-chain liquid crystalline polymer,[16c,32] and it is thus of interest to examine how the chain rigidity will affect the mesomorphic properties of the polypropiolates.

Figure 6 shows DSC thermograms of the polypropiolates. Polymer **1**-Mo entered the smectic A phase at ~141 °C during the first cooling cycle. The temperature range for the SmA mesophase was wide (~70 °C), and the polymer solidified at ~74 °C. The mesomorphic transitions was found to be enantiotropic, as the DSC thermogram recorded in the second heating scan showed k(g)-SmA and SmA-i endotherms at ~75 and ~146 °C, respectively. It should be pointed out that a polyacetylene undergoes a glass transition normally at >150 °C and often at ~200 °C.[3b,c] The low T_g (~74−75 °C) of **1** observed here is probably caused by liquation of the mesogenic pendants.[32,33] In other words, the glass transition of **1** is inherently associated with the melting of the mesogens, or $T_g = T_m$ in this system.[34] It is noteworthy that the difference between the T_m's (or T_g's) detected during the heating and cooling scans was very small (<2 °C). Most of the rigid polypropiolate main chains may have probably maintained their conformations in the neighborhood of the mesogen liquation (or glass transition) temperatures, and the ordering of the mesogenic pendants thus could be realized by a small extent of supercooling. The transition profiles of **1**-Rh were similar to those of **1**-Mo, with the i-SmA and SmA-k(g) transitions occurring at ~147 and 76 °C, respectively.[35] The transition peaks recorded during the second heating scan were roughly mirror images of those recorded during the first cooling scan with slight

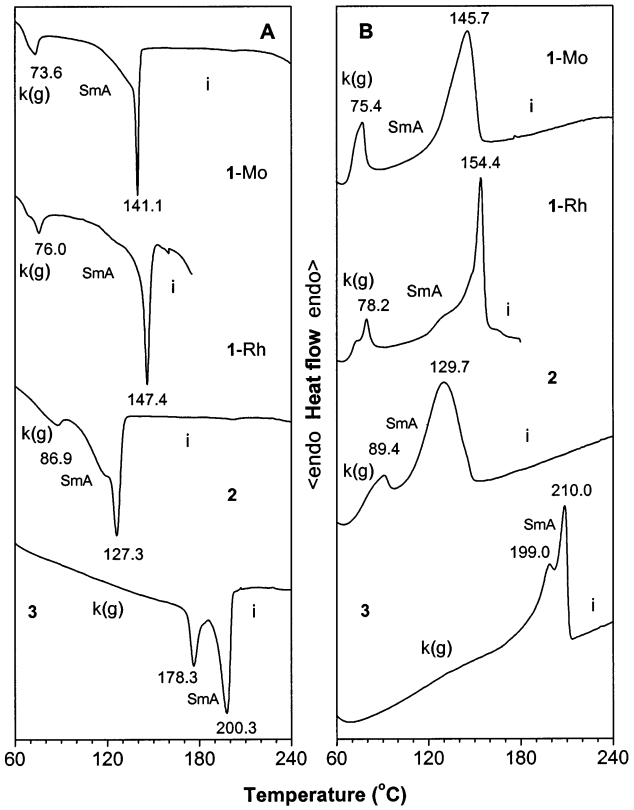

Figure 6. DSC thermograms of the mesomorphic polypropiolates **1**-Mo (sample from Table 2, no. 8), **1**-Rh (Table 2, no. 1), **2** (Table 3, no. 5), and **3** (Table 4, no. 5) recorded under nitrogen during the (A) first cooling and (B) second heating scans at a scan rate of 10 °C/min. Abbreviations: k = crystalline state, g = glassy state, SmA = smectic A phase, i = isotropic liquid.

shifts to higher temperatures, demonstrative of enantiotropic nature of the thermal transitions.

Polymer **2**, which is a structural cousin of **1** with its hydrogen atom replaced by a methyl group, also exhibited SmA mesophase and underwent enantiotropic phase transitions. The temperature range of the mesophase became, however, narrower (~40 °C). The smecticity range became even narrower (11−22 °C) when a bulkier phenyl ring was introduced to the β position in the polypropiolate structure. The increment in the chain rigidity from **1** to **3** may have progressively distorted the packing arrangements of the mesogenic pendants, which in turn decreases the stability of the SmA mesophase and narrows the mesomorphic temperature range. The structurally perturbed mesophase may be susceptible to thermal agitation and readily melted upon further heating. The melted mesogens may dissolve the polymer chains and cause isotropization to occur at "lower" temperatures. This may explain why the T_i's of **2** are lower than those of **1**. The polymer chain of **3** is, however, so rigid that its segmental movement must be activated by a high-temperature agitation even with the aid of the mesogen melting process. The T_g of **3** is thus very high, getting closer to the genuine value of T_g for a typical disubstituted polyacetylene {e.g., T_g of poly(1-phenyl-1-octyne) $-[(C_6H_5)C{=}C(C_6H_{13})]_n-$: ~200 °C[3b]}. The SmA structure of **3** was greatly distorted and underwent isotropization by a slight further heating [$T_i - T_g$ (ΔT) ~ 20 °C].

Figure 7 shows POM microphotographs of the mesomorphic textures of the polypropiolates. When the isotropic liquid of **1**-Mo was cooled to 145 °C, many small bâtonnets started to emerge from the dark background. The bâtonnets grew to bigger domains when the sample was further cooled. Lowering the temperature encouraged the growth of the bâtonnets; coalescence of the anisotropic domains resulted in the formation of focal−conic fan texture of SmA phase (Figure 7A). Typical fan texture was, however, not formed by **1**-Rh. It is known that stereoregularity makes polymer chains rigid and hampers the packing of mesogenic pendants. The stereoregular chains of **1**-Rh may have not been fully randomized by the incomplete isomerization at the isotropization temperature,[36] and the parts of regular chain segments may have obstructed the mesogens from forming a focal−conic fan texture. The fan texture was formed when the isotropic liquid of **2** was cooled, but cooling the liquid of **3** only gave an atypical birefringent texture, from which the exact nature of the mesophase was difficult to identify. With the aid of X-ray diffraction (XRD) measurements, the texture was, however, found to be associated with an SmA mesophase (vide post).

The thermal transitions and their corresponding enthalpy and entropy changes of the polypropiolates are summarized in Table 5. The large ΔH and ΔS changes involved in the SmA ↔ i transitions support the assignment of smecticity to the mesophases because those involved in the n ↔ i transitions are much smaller.[12,32] The thermal transition temperatures $T_{m(g)}$ and T_i of **1**-Rh were slightly higher than those of **1**-Mo, probably because **1**-Rh was not fully isomerized to a completely irregular structure.[16b,37] The T_g values of the polypropiolate $-[RC{=}C(CO_2R')]_n-$ increased when its structure changed from mono- to disubstitution: ~74−78 °C for **1** (R = H), ~87−89 °C for **2** (R = CH_3), and ~178−199 °C for **3** (R = C_6H_5). This trend is in agreement with our early observation for the T_g changes in nonmesomorphic substituted polyacetylenes; for example, T_g changes from 170 °C for $-\{HC{=}C[CH(SiMe_3)C_5H_{11}]\}_n-$ (monosubstituted) to 180 °C for $-[(CH_3)C{=}C(C_5H_{11})]_n-$ (disubstituted with a CH_3 substituent) and to ~200 °C for $-[(C_6H_5)C{=}C(C_6H_{13})]_n-$ (disubstituted with a bulkier C_6H_5 substituent).[3b]

We carried out XRD measurements with the aim of collecting more information on, and gaining some insights into, the molecular arrangements and packing modes in the mesophases of the polypropiolate liquid crystals. The XRD diffractogram of **1**-Mo showed a sharp reflection at a low 2θ angle (3.05°), from which a d-spacing of 28.95 Å was derived using the Bragg law $2d \sin\theta = n\lambda$ (Figure 8). The existence of the long-range order in the polymer rules out the possibility of nematic classification and reinforces the smectic assignment.[38] The calculated length of one constitutional repeat unit in **1** is 29.97 Å, which is close to the experimentally obtained layer thickness (Table 6). The mesogenic pendants of **1** are thus packed in a regular monolayer structure. The mesogens are packing so well that its high-order secondary reflection at a middle angle (2θ = 5.95°) was readily detected by the diffractometer. The peak centered at 2θ = 20.35° corresponded to the spacing between the mesogenic pendants within the layer. Different from the diffuse halos observed at the high angles in the XRD diffractograms of the liquid crystalline poly(cyanoalkyne)s we previously developed,[16d] the peak here is narrower and more intense, suggestive of better packing of the mesogens in the polypropiolate.

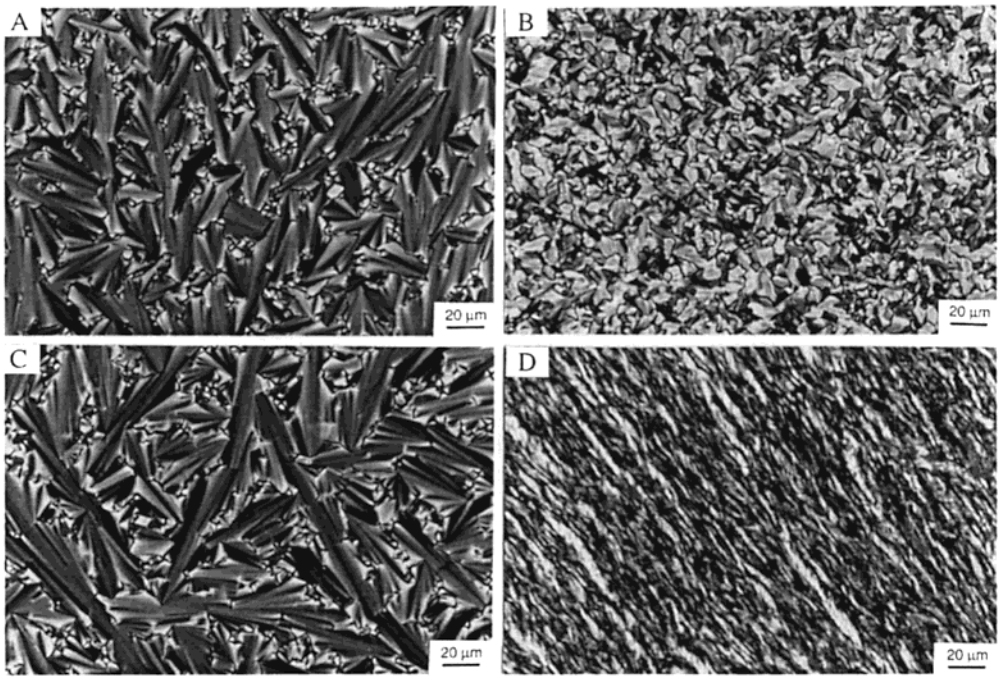

Figure 7. Mesomorphic textures observed on cooling (A) **1**-Mo (sample from Table 2, no. 8) to 123 °C, (B) **1**-Rh (Table 2, no. 1) to 115 °C, (C) **2** (Table 3, no. 5) to 100 °C, and (D) **3** (Table 4, no. 5) to 188 °C from their isotropic melts.

Table 5. Thermal Transitions and Corresponding Thermodynamic Parameters of Polypropiolates[a]

	T, °C [Δ*H*, kJ/mru; Δ*S*, J/(mru K)][b]	
polymer	cooling	heating
1-Mo	i 141.1 (−5.76; −13.91) SmA 73.6 (−1.55; −4.47) k(g)	k(g) 75.4 (1.17; 3.36) SmA 145.7 (6.52; 15.57) i
1-Rh	i 147.4 (−4.36; −10.37) SmA 76.0 (−0.82; −2.35) k(g)	k(g) 78.2 (1.26; 3.59) SmA 154.4 (4.09; 9.57) i
2	i 127.3 (−6.08; −15.12) SmA 86.9 (−1.07; −2.97) k(g)	k(g) 89.4 (1.03; 2.84) SmA 129.7 (7.59; 18.85) i
3	i 200.3 (−3.34; −7.06) SmA 178.3 (−1.28; −2.84) k(g)	k(g) 199.0 (−) SmA 209.7 (5.95; 12.33)[c] i

[a] Data taken from the DSC thermograms recorded under nitrogen in the first cooling and second heating scans; abbreviations: k = crystalline state, g = glassy state, SmA = smectic A phase, i = isotropic liquid. [b] Abbreviation: mru = monomer repeat unit. [c] Sum of overlapping transitions.

Similarly, **1**-Rh showed Bragg reflections in the low- and high-angle regions, from which *d*-spacings corresponding to the monolayer structure could be derived. The reflections were, however, weaker and broader, confirming that the stereoregular chain segments hamper the ordering of mesogenic pendants. Polymer **2** exhibited a weak reflection on the most left side of its diffractogram. The second reflection at $2\theta = 5.65°$ ($d = 15.63$ Å) was, however, strong. Similar phenomena have been observed in other systems,[39] although we do not know the cause for this in our system at present. No primary reflection peak was observed in the diffractogram of **3** in the low angle region, and the reflections owing to the packings of the heptyloxybiphenylcarbonyloxy and biphenyl pendants were detected at $2\theta = 5.4°$ ($d = 16.36$ Å) and 8.2° ($d = 10.77$ Å), respectively. The broadness of those peaks, the lack of the primary reflection, and the low d_2/l_2 ratio (Table 6) demonstrate the poor layer packing arrangements in **3**, which may account for the difficulty for the polymer to form typical focal−conic SmA textures.

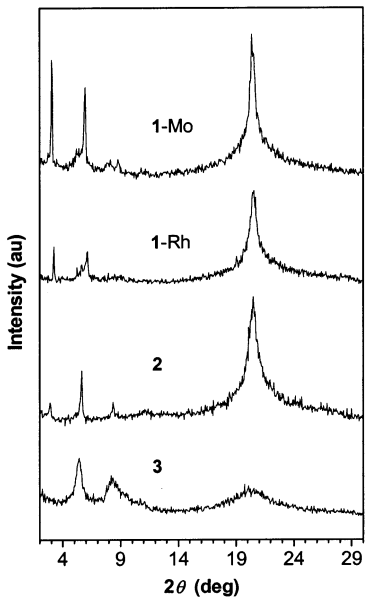

Figure 8. X-ray diffraction patterns of the mesomorphic polyacetylenes quenched by liquid nitrogen from their liquid crystalline states: **1**-Mo (sample from Table 2, no. 8) at 135 °C, **1**-Rh (Table 2, no. 1) at 130 °C, **2** (Table 3, no. 5) at 120 °C, and **3** (Table 4, no. 5) at 200 °C.

Electronic Absorption and Light Emission. The absorption spectra of the polypropiolates are given in Figure 9. Polymer **1**-Mo exhibited a strong K-band of the biphenyl chromophore at 295 nm. Little absorption was observed in the long wavelength region, suggesting

Table 6. X-ray Diffraction Analysis Data for Polypropiolates[a]

polymer	T (°C)	d_1 (Å)	d_2 (Å)	d_3 (Å)	d_4 (Å)	ratio d_1/l_1[b]	ratio d_2/l_2[c]	mesophase
1-Mo	135	28.95	14.85		4.36	0.97		SmA
1-Rh	130	27.16	14.36		4.32	0.91		SmA
2	120	30.44	15.63	10.58	4.33	0.95		SmA
3	200		16.36	10.77	4.41		0.88	SmA

[a] The mesomorphic structures in the liquid crystalline states at the given temperatures were frozen by the rapid quenching with liquid nitrogen. [b] l_1: calculated length of the constitutional repeat unit in its fully extended conformation. [c] l_2: length of the heptyloxybiphenylcarbonyloxy mesogen.

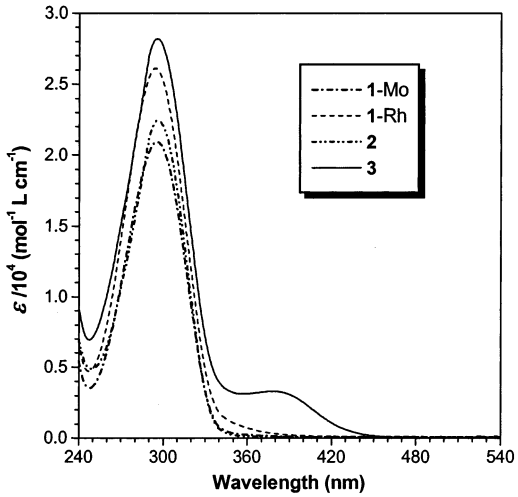

Figure 9. UV−vis spectra of THF solutions of **1**-Mo (sample from Table 2, no. 8), **1**-Rh (Table 2, no. 1), **2** (Table 3, no. 5), and **3** (Table 4, no. 5).

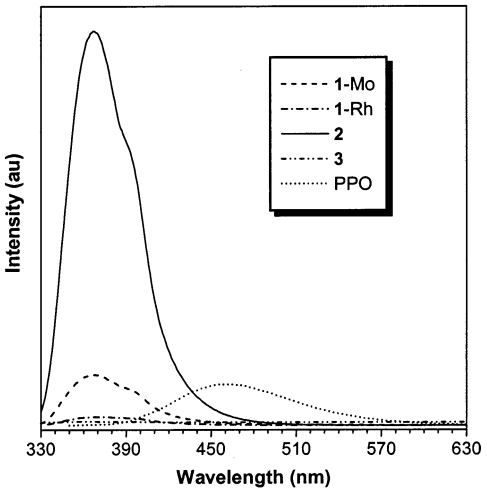

Figure 10. Fluorescence spectra of THF solutions of **1**-Mo (sample from Table 2, no. 8), **1**-Rh (Table 2, no. 1), **2** (Table 3, no. 5), and **3** (Table 4, no. 5). The spectrum of poly(1-phenyl-1-octyne) (PPO) is shown for comparison. Concentration: 0.05 mM; excitation wavelength (nm): 333 (**1**−**3**), 355 (PPO).

that the polymer possesses a short persistence length of backbone conjugation. Polymer **1**-Rh exhibited not only a more intense K-band of biphenyl pendant at 295 nm but also a stronger backbone absorption in the longer wavelength region. We have previously found that the electronic absorption of a polyacetylene chain increases with its stereoregularity.[16b] The regular stereostructure of **1**-Rh may allow its biphenyl pendant and polyene backbone to take comparatively more planar conformations and hence make them more absorptive. The replacement of the β hydrogen in **1** by a methyl group did not alter its ground-state electronic transitions: the absorption spectrum of **2** was similar to that of **1**-Mo.[40] Polymer **3**, however, absorbed intensely at 295 nm. This enhanced absorption is probably due to the additional contribution from its constitutional repeat unit of $-C_6H_5C{=}CCO_2R-$, which is not only conjugated[41] but also polarized by the intramolecular push−pull interaction. The backbone absorption of **3** was clearly observed at ∼380 nm. Unlike the methyl group in **2**, the phenyl substituent in **3** is a planar ring. As proposed by Ginsburg, Gorman, and Grubbs, the steric requirements of aromatic substituents may enforce a planar conformation of polyacetylene backbone.[2c] The planar backbone allows better conjugation of the alternating double bonds and hence makes the polymer absorptive in the longer wavelength region.

It is known that light-emitting efficiency of a substituted polyacetylene with chromophoric pendants (Ch) is sensitive to its molecular structure: a monosubstituted poly(1-arylacetylene) of general structure $-[HC{=}C(Ar-Ch)]_n-$ is weakly luminescent, a poly(1-alkylacetylene) $-\{HC{=}C[(CH_2)_m-Ch]\}_n-$ can be highly emissive, and a disubstituted poly(1-aryl-1-alkyne) $-\{(Ar)C{=}C[(CH_2)_m-Ch]\}_n-$ is normally a good emitter.[20] We were intrigued to know whether this structure−property relationship also holds for the light emission of polypropiolates. To address this basic question, we investigated their fluorescence behaviors. Dilute solutions of the polypropiolates (50 μM) were used in an effort to avoid possible complications from the nonmolecular species such as physical aggregates that are often formed in the solid films of conjugated organics and polymers.[42,43]

When polymer **1**-Mo was photoexcited at 333 nm, it emitted a UV light of 369 nm (Figure 10). Its maximum emission intensity was comparable to that of poly(1-phenyl-1-octyne) (PPO), a well-known highly luminescent disubstituted polyacetylene,[20,44,45] but its quantum yield (Φ_F = 0.16) was lower than that of PPO (0.43). The emission from its stereoregular cousin **1**-Rh was, however, very weak, whose quantum yield was as low as 0.0085. Stereoregular chains have been found to be detrimental to light emission in many conjugated polymer systems;[46,47] the same is true for the photoluminescence of the polypropiolate, as proved by the observation here that the Φ_F of the stereoregular **1**-Rh was ∼20-fold lower than that of the stereoirregular **1**-Mo. The disubstituted polymer **2** emitted a very strong UV light with a quantum yield as high as 0.70. Astonishingly, however, polymer **3** was nearly nonluminescent. This is probably caused by a self-quenching mechanism. The emission spectrum of the biphenyl pendants of **3** overlaps with the absorption spectrum of its polypropiolate backbone (cf. Figure 9), and the UV light emitted from the pendants is absorbed by the nonemissive backbone—this unfavorable energy transfer effectively quenched the light emission of the polymer.

We have previously observed that the emission efficiency (Φ_F) of a series of polyacetylenes of general structure $-\{RC{=}C[(CH_2)_m-Ch]\}_n-$ changes with R in the following order: $\Phi_{F,Me} > \Phi_{F,Ph} > \Phi_{F,H}$.[20,48,49] Gener-

ally, a disubstituted polymer performs better as a light emitter than its monosubstituted congener, due to the reduction in interchain interactions caused by the better chain separation in the disubstituted polymer system.[20,44,45] What we observed here for polypropiolate $-\{RC{=}C[CO_2(CH_2)_6{-}Ch]\}_n-$ is, however, $\Phi_{F,Me}$ (**2**) > $\Phi_{F,H}$ (**1**) > $\Phi_{F,Ph}$ (**3**). Compared with the order in the $-\{RC{=}C[(CH_2)_m{-}Ch]\}_n-$ system, the order of $\Phi_{F,H}$ vs $\Phi_{F,Ph}$ in polypropiolates is inversed. This is mainly caused by the nonluminescent nature of the polyphenylpropiolate backbone. While the polyphenylalkyne backbone in $-\{PhC{=}C[(CH_2)_m{-}Ch]\}_n-$ is emissive, the electronic interaction of the propiolic carbonyloxy group with the polyene double bond makes the polyphenylpropiolate backbone in $-\{RC{=}C[CO_2(CH_2)_6{-}Ch]\}_n-$ an effective quenching site.

Concluding Remarks

In this work, we synthesized a group of new functional substituted polypropiolates and studied their thermal, mesogenic, and luminescent properties. Our results and findings can be summarized as follows.

(1) The polymerizations of monosubstituted propiolate **8** were effected by both the Rh and Mo catalysts, with the former giving stereoregular polymeric products. The disubstituted propiolates **9** and **10** could, however, only be polymerized by the Mo catalysts. These monomers are the first examples of substituted propiolates that are effectively polymerized by the inexpensive "classic" metathesis catalyst of $MoCl_5$.

(2) All the polypropiolates were thermally stable and started to lose their weights at temperatures as high as ≥350 °C, irrespective of whether they were mono- or disubstituted, thanks to the synergistic interplay of the electron-withdrawing effect of the propiolic carbonyloxy group and the jacket effect of the aromatic (biphenyl) pendant.[16b,c,50]

(3) Both the mono- and disubstituted polypropiolates were liquid crystalline and formed a monolayered smectic mesophase at appropriate temperatures. The chain stereoregularity and backbone rigidity were found to be detrimental to the mesogenic packing in the formation of the SmA phase.

(4) The stereoregular chain of **1** was unable to emit, and the poly(phenylpropiolate) backbone of **3** was nonluminescent. The poly(methylpropiolate) **2** was, however, highly emissive, whose quantum yield was more than 1.5-fold higher than that of PPO, a well-known light-emitting disubstituted polyacetylene.

A wide variety of mesomorphic monosubstituted polyacetylenes have been developed,[11−22,51] but their disubstituted counterparts are still rare species. The polypropiolates **2** and **3** belong to this rare category of liquid crystalline disubstituted polyacetylenes. Polymer **2** is of particular interest because it also emits strong UV light. The mesomorphism and luminescence of the polymer, coupled with its high thermal stability, make it a promising candidate for specialty materials; for example, its aligned films may be utilized as a polarized light source in the construction of optical display systems.

Experimental Section

Materials. The (substituted) propiolic acids **6**, i.e., propiolic acid, 2-butynoic acid (or tetrolic acid), and phenylpropiolic acid, were purchased from Aldrich and used as received. Dioxane (Nacalai Tesque) and toluene (BDH) were predried over 4 Å molecular sieves and distilled from sodium benzophenone ketyl immediately prior to use. Dichloromethane (Lab-Scan) was dried over molecular sieves and distilled from calcium hydride. Except for molybdenum(V) chloride (Acros), all the other commercially available reagents and solvents were purchased from Aldrich and used without further purification. The organorhodium catalysts and 6-hydroxy-1-hexyl (4-heptyloxy-4-biphenylyl)carboxylate mesogen (**7**) were prepared according to our previously described procedures.[24,52]

Instrumentation. The IR spectra were measured on a Perkin-Elmer 16 PC FT-IR spectrophotometer. The ^1H and ^{13}C NMR spectra were recorded on a Bruker ARX 300 spectrometer using chloroform-*d* as solvent and tetramethylsilane ($\delta = 0$) or chloroform (7.26) as internal reference. The UV spectra were measured on a Milton Roy Spectronic 3000 array spectrophotometer, and the molar absorptivity (ϵ) of the polymers was calculated on the basis of their monomer repeat units. The mass spectra were recorded on a Finnigan TSQ 7000 triple quadrupole mass spectrometer operating in a chemical ionization (CI) mode using methane as carrier gas. The molecular weights of the polymers were estimated by a Waters Associates GPC system. Degassed THF was used as eluent at a flow rate of 1.0 mL/min. A set of monodisperse polystyrene standards covering the molecular weight range of 10^3-10^7 Da was used for the molecular weight calibration.

The thermal stability of the polymers was evaluated on a Perkin-Elmer TGA 7 under nitrogen at a heating rate of 10 °C/min. A Perkin-Elmer DSC 7 was used to record the phase transition thermograms. An Olympus BX 60 POM equipped with a Linkam TMS 92 hot stage was used to observe anisotropic optical textures. The XRD patterns were recorded on a Philips PW1830 powder diffractometer with a graphite monochromator using 1.5406 Å Cu Kα wavelength at room temperature (scanning rate 0.05°/s, scan range 2−30°). The polymer samples for the XRD measurements were prepared by freezing the molecular arrangements in the liquid crystalline states by liquid nitrogen as previously reported.[11,12]

Monomer Synthesis. The mesogenic propiolates **8**−**10** were synthesized by esterification of **7** with **6** in the presence of DCC, TsOH, and DMAP. A detailed experimental procedure for the synthesis of **8** is given below as an example.

6-{[(4′-Heptyloxy-4-biphenylyl)carbonyl]oxy}hexylpropiolate (8). In a typical run, 3.5 g (8.5 mmol) of **7**, 2.6 g (12.8 mmol) of DCC, 0.3 g (1.7 mmol) of TsOH, and 0.2 g (1.7 mmol) of DMAP were dissolved in 200 mL of dry CH_2Cl_2 in a 500 mL, two-necked flask in an atmosphere of nitrogen. The solution was cooled to 0−5 °C with an ice−water bath, to which 0.7 g (10.2 mmol) of propiolic acid dissolved in 50 mL of CH_2Cl_2 was added under stirring via a dropping funnel. The reaction mixture was stirred overnight. After filtering out the formed urea solid, the solution was concentrated by a rotary evaporator. The crude product was purified by a silica gel column using chloroform as eluent. Recrystallization in an ethanol/H_2O mixture (4:1 by volume) gave 3.0 g of white solid (yield: 76.5%). IR (KBr), ν (cm^{-1}): 3245 (s, HC≡), 2113 (vs, C≡C), 1702 (vs, C═O). ^1H NMR (300 MHz, $CDCl_3$), δ (ppm): 8.07 (d, 2H, Ar−H ortho to CO_2), 7.63 (d, 2H, Ar−H meta to CO_2), 7.54 (d, 2H, Ar−H meta to OC_7H_{15}), 6.98 (d, 2H, Ar−H ortho to OC_7H_{15}), 4.33 (t, 2H, $ArCO_2CH_2$), 4.21 (t, 2H, $\equiv CCO_2CH_2$), 4.00 (t, 2H, OCH_2), 2.88 (s, 1H, H−C≡), 1.80−1.72 (m, 4H, $ArCO_2CH_2CH_2$ and $\equiv CCO_2CH_2CH_2$), 1.50−1.32 [m, 14 H, $(CH_2)_7$], 0.90 (t, 3H, CH_3). ^{13}C NMR (75 MHz, $CDCl_3$), δ (ppm): 166.4 ($ArCO_2$), 159.3 (aromatic carbon linked with OC_7H_{15}), 152.6 ($\equiv CCO_2$), 145.5 (aromatic carbons para to CO_2), 131.9 (aromatic carbons para to OC_7H_{15}), 129.9 (aromatic carbons ortho to CO_2), 128.2 (aromatic carbons meta to OC_7H_{15}), 128.1 (aromatic carbon linked with CO_2), 126.2 (aromatic carbons meta to CO_2), 114.7 (aromatic carbons ortho to OC_7H_{15}), 74.60 (HC≡), 74.57 (≡C), 67.9 (OCH_2), 66.1 ($ArCO_2CH_2$), 64.6 ($\equiv CCO_2CH_2$), 31.6, 29.1, 28.9, 28.5, 28.1, 25.9, 25.6, 25.4, 22.5, 14.0. MS (CI): *m/e* 464.1 [$(M + 1)^+$, calcd 464.1].

6-{[(4′-Heptyloxy-4-biphenylyl)carbonyl]oxy}hexyl-2-butynate (9). The monomer was prepared by a procedure similar to that described above for the preparation of **8**. White

solid; yield 82.3%. IR (KBr), ν (cm^{-1}): 2246 (vs, C≡C), 1709 (vs, C═O). ^1H NMR (300 MHz, $CDCl_3$), δ (ppm): 8.07 (d, 2H, Ar−H ortho to CO_2), 7.62 (d, 2H, Ar−H meta to CO_2), 7.56 (d, 2H, Ar−H meta to OC_7H_{15}), 6.98 (d, 2H, Ar−H ortho to OC_7H_{15}), 4.33 (t, 2H, $ArCO_2CH_2$), 4.21 (t, 2H, ≡CCO_2CH_2), 4.00 (t, 2H, OCH_2), 1.98 (s, 3H, CH_3C≡), 1.81−1.71 (m, 4H, $ArCO_2CH_2CH_2$ and ≡$CCO_2CH_2CH_2$), 1.48−1.33 [m, 14 H, $(CH_2)_7$], 0.90 (t, 3H, CH_3). ^{13}C NMR (75 MHz, $CDCl_3$), δ (ppm): 166.5 ($ArCO_2$), 159.4 (aromatic carbon linked with OC_7H_{15}), 153.8 (≡CCO_2), 145.1 (aromatic carbons para to CO_2), 132.0 (aromatic carbons para to OC_7H_{15}), 130.0 (aromatic carbons ortho to CO_2), 128.4 (aromatic carbons meta to OC_7H_{15}), 128.2 (aromatic carbon linked with CO_2), 126.3 (aromatic carbons meta to CO_2), 114.9 (aromatic carbons ortho to OC_7H_{15}), 85.3 (CH_3C≡), 72.4 (≡CCO_2), 68.1 (OCH_2), 65.6 ($ArCO_2CH_2$), 64.7 (≡CCO_2CH_2), 31.7, 29.2, 29.0, 28.6, 28.3, 25.9, 25.7, 25.5, 22.5, 14.0, 3.7 (CH_3C≡). MS (CI): *m/e* 478.1 [$(M + 1)^+$, calcd 478.2].

6-{[(4′-Heptyloxy-4-biphenylyl)carbonyl]oxy}hexylphenylpropiolate (10). Its synthetic procedure is similar to that of **8**. White solid; yield 81.5%. IR (KBr), ν (cm^{-1}): 2221 (vs, C≡C), 1705 (vs, C═O). ^1H NMR (300 MHz, $CDCl_3$), δ (ppm): 8.07 (d, 2H, Ar−H ortho to CO_2), 7.63−7.54 (m, 6H, Ar−H meta to CO_2, Ar−H meta to OC_7H_{15}, and Ar−H ortho to C≡C), 7.37 (m, 3H, Ar−H meta and para to C≡C), 6.98 (d, 2H, Ar−H ortho to OC_7H_{15}), 4.35 (t, 2H, $ArCO_2CH_2$), 4.26 (t, 2H, ≡CCO_2CH_2), 4.00 (t, 2H, OCH_2), 1.83−1.77 (m, 4H, $ArCO_2CH_2CH_2$ and ≡$CCO_2CH_2CH_2$), 1.52−1.33 [m, 14 H, $(CH_2)_7$], 0.90 (t, 3H, CH_3). ^{13}C NMR (75 MHz, $CDCl_3$), δ (ppm): 166.4 ($ArCO_2$), 159.2 (aromatic carbon linked with OC_7H_{15}), 154.0 (≡CCO_2), 145.1 (aromatic carbons para to CO_2), 132.8 (aromatic carbons ortho to C≡C), 132.0 (aromatic carbons para to OC_7H_{15}), 130.5 (aromatic carbons para to C≡C), 130.0 (aromatic carbons ortho to CO_2), 128.2 (aromatic carbons meta to OC_7H_{15}), 128.1 (aromatic carbon linked with CO_2), 126.2 (aromatic carbons meta to CO_2), 119.5 (aromatic carbon linked with C≡C), 114.9 (aromatic carbons ortho to OC_7H_{15}), 86.0 (ArC≡), 80.6 (≡CCO_2), 68.0 (OCH_2), 65.9 ($ArCO_2CH_2$), 64.7 (≡CCO_2CH_2), 31.7, 29.1, 29.0, 28.5, 28.3, 25.9, 25.6, 25.5, 22.5, 14.0. MS (CI): *m/e* 540.1 [$(M + 1)^+$, calcd 540.3].

Polymerization. All the polymerization reactions and manipulations were carried out under nitrogen using Schlenk techniques in a vacuum line system or in an inert-atmosphere glovebox (Vacuum Atmospheres), except for the purification of the polymers, which was done in an open atmosphere. A typical experimental procedure for the polymerization of **8** is given below.

Into a baked 20 mL Schlenk tube with a stopcock in the sidearm was added 360.0 mg (0.77 mmol) of **8**. The tube was evacuated under vacuum and then flushed with dry nitrogen three times through the sidearm. Freshly distilled toluene (2 mL) was injected into the tube to dissolve the monomer. The catalyst solution was prepared in another tube by dissolving 11.0 mg of $MoCl_5$ and 17.0 mg of Ph_4Sn in 2 mL of toluene. The two tubes were aged at 60 °C for 15 min, and the monomer solution was transferred to the catalyst solution using a hypodermic syringe. The polymerization mixture was stirred under nitrogen for 24 h. The solution was then cooled to room temperature, diluted with 5 mL of chloroform, and added dropwise to 500 mL of acetone through a cotton filter under stirring. The precipitate was allowed to stand overnight, which was then filtered with a Gooch crucible. The polymer was washed with acetone and dried in a vacuum oven to a constant weight.

Characterization Data. 1-Mo: Gray powdery solid; yield 47.4%. M_w 23 190, M_w/M_n 2.0 (GPC; Table 2, no. 8). IR (KBr), ν (cm^{-1}): 1714 (vs, C═O). ^1H NMR (300 MHz, $CDCl_3$), δ (ppm): 7.86, 7.39, 6.80 (Ar−H, *E* H−C═, and *Z* H−C═), 4.11, 3.82 ($ArCO_2CH_2$, ═CCO_2CH_2, and OCH_2), 1.63 ($ArCO_2CH_2CH_2$ and ═$CCO_2CH_2CH_2$), 1.21 [$(CH_2)_7$], 0.80 (CH_3). ^{13}C NMR (75 MHz, $CDCl_3$), δ (ppm): 166.0 ($ArCO_2$ and ═CCO_2), 159.1 (aromatic carbon linked with OC_7H_{15}), 144.8 (aromatic carbons para to CO_2), 131.7 (═CCO_2 and aromatic carbons para to OC_7H_{15}), 129.8 (aromatic carbons ortho to CO_2), 128.0 (HC═ and aromatic carbons meta to OC_7H_{15} and linked with CO_2), 126.0 (aromatic carbons meta to CO_2), 114.6 (aromatic carbons ortho to OC_7H_{15}), 67.8 (OCH_2), 64.6 ($ArCO_2CH_2$), 31.6, 29.1, 28.9, 28.5, 25.8, 25.5, 22.4, 13.9. UV (THF, 10.08×10^{-5} mol/L), $\lambda_{max}/\epsilon_{max}$: 295 nm/$2.09 \times 10^4$ mol^{-1} L cm^{-1}.

1−Rh: The polymer was prepared by $[Rh(nbd)Cl]_2$ catalyst in acetonitrile at 40 °C using a procedure similar to that described above. Orange powdery solid; yield 40.3%. M_w 353 600, M_w/M_n 2.7 (GPC; Table 2, no. 1). IR (KBr), ν (cm^{-1}): 1715 (vs, C═O). ^1H NMR (300 MHz, $CDCl_3$), δ (ppm): 7.86, 7.83, 7.39, 7.30, 7.26, 6.80, 6.74 (Ar−H, *E* H−C═, and *Z* H−C═), 4.13, 3.83, 3.70 ($ArCO_2CH_2$, ═CCO_2CH_2, and OCH_2), 1.62, 1.53 ($ArCO_2CH_2CH_2$ and ═$CCO_2CH_2CH_2$), 1.21 [$(CH_2)_7$], 0.80 (CH_3). ^{13}C NMR (75 MHz, $CDCl_3$), δ (ppm): 166.2 ($ArCO_2$ and ═CCO_2), 159.2 (aromatic carbon linked with OC_7H_{15}), 144.6 (aromatic carbons para to CO_2), 131.9 (═CCO_2 and aromatic carbons para to OC_7H_{15}), 129.9 (aromatic carbons ortho to CO_2), 128.0 (HC═ and aromatic carbons meta to OC_7H_{15} and linked with CO_2), 126.1 (aromatic carbons meta to CO_2), 114.7 (aromatic carbons ortho to OC_7H_{15}), 67.9 (OCH_2), 64.8 ($ArCO_2CH_2$), 31.7, 29.2, 29.1, 28.7, 26.0, 25.6, 22.6, 14.0. UV (THF, 7.80×10^{-5} mol/L), $\lambda_{max}/\epsilon_{max}$: 295 nm/$2.48 \times 10^4$ mol^{-1} L cm^{-1}.

2: Gray powdery solid; yield 44.0%. M_w 9190, M_w/M_n 2.1 (GPC; Table 3, no. 5). IR (KBr), ν (cm^{-1}): 1705 (vs, C═O). ^1H NMR (300 MHz, $CDCl_3$), δ (ppm): 8.03, 7.53, 6.92 (Ar−H), 4.28, 4.13, 3.93 ($ArCO_2CH_2$, ═CCO_2CH_2, and OCH_2), 2.2 (CH_3C═), 1.76 ($ArCO_2CH_2CH_2$ and ═$CCO_2CH_2CH_2$), 1.59, 1.30 [$(CH_2)_7$], 0.88 (CH_3). ^{13}C NMR (75 MHz, $CDCl_3$), δ (ppm): 166.2 ($ArCO_2$ and ═CCO_2), 164.3 (═CCO_2) 159.2 (aromatic carbon linked with OC_7H_{15}), 144.9 (aromatic carbons para to CO_2), 131.9 (═CCO_2 and aromatic carbons para to OC_7H_{15}), 130.5 (CH_3C═ and aromatic carbons ortho to CO_2), 128.2 (aromatic carbons meta to OC_7H_{15} and linked with CO_2), 126.1 (aromatic carbons meta to CO_2), 114.7 (aromatic carbons ortho to OC_7H_{15}), 67.9 (OCH_2), 64.6 ($ArCO_2CH_2$), 31.6, 29.1, 28.9, 28.5, 27.7, 26.0, 25.8, 25.6, 22.6,19.2 (CH_3C═), 14.0. UV (THF, 5.90×10^{-4} mol/L), $\lambda_{max}/\epsilon_{max}$: 296 nm/$2.23 \times 10^4$ mol^{-1} L cm^{-1}.

3: Yellow green powdery solid; yield 56.8%. M_w 239 300, M_w/M_n 3.2 (GPC; Table 4, no. 5). IR (KBr), ν (cm^{-1}): 1715 (vs, C═O). ^1H NMR (300 MHz, $CDCl_3$), δ (ppm): 8.00, 7.51, 6.92, 6.65 (Ar−H), 4.25, 3.94 ($ArCO_2CH_2$, ═CCO_2CH_2, and OCH_2), 1.77 ($ArCO_2CH_2CH_2$ and ═$CCO_2CH_2CH_2$), 1.31 [$(CH_2)_7$], 0.890 (CH_3). ^{13}C NMR (75 MHz, $CDCl_3$), δ (ppm): 166.2 ($ArCO_2$ and ═CCO_2), 159.1 (aromatic carbon linked with OC_7H_{15}), 144.8 (aromatic carbons para to CO_2), 131.8 (═CCO_2 and aromatic carbons para to OC_7H_{15}), 129.8 (C_6H_5C═ and aromatic carbons ortho to CO_2), 128.0 (aromatic carbons meta to OC_7H_{15} and linked with CO_2), 126.1 (aromatic carbons meta to CO_2), 114.6 (aromatic carbons ortho to OC_7H_{15}), 67.9 (OCH_2), 64.5 ($ArCO_2CH_2$), 31.6, 29.1, 28.9, 28.5, 25.8, 25.6, 22.4, 13.9. UV (THF, 5.90×10^{-4} mol/L), $\lambda_{max}/\epsilon_{max}$: 296 nm/$2.80 \times 10^4$ mol^{-1} L cm^{-1}.

Acknowledgment. The work described in the paper was partially supported by the Research Grants Council of the Hong Kong Special Administrative Region, China (Project Nos. HKUST 6187/99P, 6121/01P, and 6085/02P) and the University Grants Committee of Hong Kong through an Area of Excellence Scheme (Project No. AoE/P-10/01-1-A).

References and Notes

(1) For recent reviews, see: (a) Shirakawa, H. *Angew. Chem., Int. Ed.* **2001**, *40*, 2575−2580. (b) MacDiarmid, A. G. *Angew. Chem., Int. Ed.* **2001**, *40*, 2581−2590. (c) Heeger, A. J. *Angew. Chem., Int. Ed.* **2001**, *40*, 2591−2611.

(2) For selected reviews, see: (a) Masuda, T.; Higashimura, T. *Adv. Polym. Sci.* **1987**, *81*, 121. (b) Gibson, H. W.; Pochan, J. M. In *Concise Encyclopedia of Polymer Science and Engineering*; Kroschwitz, J. I., Ed.; Wiley: New York, 1990; pp 7−9. (c) Ginsburg, E. J.; Gorman, C. B.; Grubbs, R. H. In *Modern Acetylene Chemistry*; Stang, P. J., Diederich, F., Eds.; VCH: New York, 1995; Chapter 10, pp 353−383. (d) Tabata, M.; Sone, T.; Sadahiro, Y. *Macromol. Chem. Phys.* **1999**, *200*, 265−282. (e) Reddinger, J. L.; Reynolds, J. R. *Adv. Polym.*

Sci. **1999**, *145*, 57−122. (d) Volidal, J.; Sedlacek, J. In *Chromatography of Polymers: Hyphenated and Multidimensional Techniques*; Provder, T., Ed.; ACS Symposium Series 731; American Chemical Society: Washington, DC, 1999; Chapter 19, pp 263−287.

(3) (a) Masuda, T.; Tang, B. Z.; Higashimura, T.; Yamaoka, H. *Macromolecules* **1985**, *18*, 2369−2373. (b) Masuda, T.; Tang, B. Z.; Tanaka, T.; Higashimura, T. *Macromolecules* **1986**, *19*, 1459−1464. (c) Seki, H.; Tang, B. Z.; Tanaka, A.; Masuda, T. *Polymer* **1994**, *35*, 3456−3462. (d) Karim, S. M.; Nomura, R.; Masuda, T. *J. Polym. Sci., Part A: Polym. Chem.* **2001**, *39*, 3130−3136.

(4) (a) Daranga, M.; Bulacovschi, V.; Mihailescu, C. *Eur. Polym. J.* **1990**, *26*, 117−120. (b) Nishide, H.; Yoshioka, N.; Inagaki, K.; Kaku, T.; Tsuchida, E. *Macromolecules* **1992**, *25*, 569−575. (c) Lee, H. J.; Shim, S. C. *J. Chem. Soc., Chem. Commun.* **1993**, 1420−1422. (d) Gal, Y.-S. *J. Macromol. Sci., Pure Appl. Chem.* **1994**, *A31*, 703−714. (d) Gal, Y.-S. *J. Macromol. Sci., Pure Appl. Chem.* **1994**, *A32*, 61−72.

(5) Masuda, T.; Kawai, M.; Higashimura, T. *Polymer* **1982**, *23*, 744−747.

(6) (a) Ho, T. H.; Katz, T. J. *J. Mol. Catal.* **1985**, *28*, 359−367. (b) Rossitto, F. C.; Lahti, P. M. *Macromolecules* **1993**, *26*, 6308−6309.

(7) (a) Nishida, M.; Fujii, S.; Aoki, T.; Hayakama, Y.; Muramatsu, H.; Morita, T. *J. Fluorine Chem.* **1990**, *46*, 445−459. (b) Tabata, M.; Tanaka, Y.; Sadahiro, Y.; Sone, T.; Yokota, K.; Miura, I. *Macromolecules* **1997**, *30*, 5200−5204.

(8) (a) Katz, T. J.; Lee, S. J. *J. Am. Chem. Soc.* **1980**, *102*, 422−424. (b) Gal. Y.-S.; Jung, B.; Lee, W.-C.; Choi, S.-K. *J. Polym. Sci., Part A: Polym. Chem.* **1992**, *30*, 2657−2662.

(9) Calini, C.; Chien, J. C. W. *J. Polym. Sci., Polym. Chem. Ed.* **1984**, *22*, 2749−2766.

(10) Gai, Y.-S. *J. Chem. Soc., Chem. Commun.* **1994**, 327−328.

(11) (a) Tang, B. Z.; Lam, J. W. Y.; Luo, J, D.; Dong, Y.; Cheuk, K. K. L.; Xie, Z.; Kwok, H.-S. In *Liquid Crystals V*; Khoo, I., Ed.; SPIE: Bellingham, WA, 2001; pp 132−138. (b) Tang, B. Z.; Lam, J. W. Y.; Kong, X.; Salhi, F.; Cheuk, K. K. L.; Kwok, H. S.; Huang, Y. M.; Ge, W. In *Liquid Crystals IV*; Khoo, I., Ed.; SPIE: Bellingham, WA, 2000; pp 24−30. (c) Tang, B. Z.; Lam, J. W. Y.; Kong, X.; Lee, P. P. S.; Wan, X.; Kwok, H. S.; Huang, Y. M.; Ge, W.; Chen, H.; Xu, R.; Wang, M. In *Liquid Crystals III*; Khoo, I., Ed.; SPIE: Bellingham, WA, 1999; pp 62−71.

(12) (a) Lam, J. W. Y.; Dong, Y. P.; Cheuk, K. K. L.; Luo, J. D.; Xie, Z. L.; Kwok, H. S.; Mo, Z. S.; Tang, B. Z. *Macromolecules* **2002**, *35*, 1229−1240. (b) Huang, Y. M.; Ge, W.; Lam, J. W. Y.; Cheuk, K. K. L.; Tang, B. Z. *Mater. Sci. Eng., B* **2001**, *85*, 242−246. (c) Lam, J. W. Y.; Kong, X.; Dong, Y. P.; Cheuk, K. K. L.; Xu, K.; Tang, B. Z. *Macromolecules* **2000**, *33*, 5027−5040. (d) Huang, Y. M.; Lam, J. W. Y.; Cheuk, K. K. L.; Ge, W.; Tang, B. Z. *Thin Solid Films* **2000**, *363*, 146−148. (e) Huang, Y. M.; Ge, W.; Lam, J. W. Y.; Tang, B. Z. *Appl. Phys. Lett.* **1999**, *75*, 4094−4096. (f) Huang, Y.; Bu, L.; Zhang, D.; Su, C.; Xu, Z.; Lam, J. W. Y.; Tang, B. Z. *J. Funct. Polym.* **1999**, *12*, 376−380. (g) Kong, X.; Wan, X.; Kwok, H. S.; Feng, X.-D.; Tang, B. Z. *Chin. J. Polym. Sci.* **1998**, *16*, 185−192.

(13) (a) Huang, Y. M.; Ge, W.; Lam, J. W. Y.; Tang, B. Z. *Appl. Phys. Lett.* **2001**, *78*, 1652−1654. (b) Huang, Y. M.; Ge, W.; Lam, J. W. Y.; Cheuk, K. K. L.; Tang, B. Z. *Mater. Sci. Eng., B* **2001**, *85*, 122−125. (c) Huang, Y. M.; Ge, W.; Lam, J. W. Y.; Cheuk, K. K. L.; Tang, B. Z. *Mater. Sci. Eng., B* **2001**, *85*, 118−121. (d) Huang, Y.; Bu, L. J.; Bu, L. W.; Zhang, D. Z.; Su, C. W.; Xu, Z. D.; Lam, W. Y.; Tang, B. Z.; Mays, J. W. *Polym. Bull. (Berlin)* **2000**, *44*, 539−546. (e) Huang, Y. M.; Lam, J. W. Y.; Cheuk, K. K. L.; Ge, W.; Tang, B. Z. *Macromolecules* **1999**, *32*, 5976−5978. (f) Tang, B. Z.; Kong, X.; Feng, X.-D. *Chin. J. Polym. Sci.* **1999**, *17*, 289−294. (g) Huang, M. Y. M.; Law, C. K.; Ge, W.; Lam, J. W. Y.; Tang, B. Z. *J. Lumin.* **2002**, *99*, 161−168.

(14) (a) Tang, B. Z.; Chen, H. Z.; Xu, R. S.; Lam, J. W. Y.; Cheuk, K. K. L.; Wong, H. N. C.; Wang, M. *Chem. Mater.* **2000**, *12*, 213−221. (b) Lee, P. P. S.; Geng, Y. H.; Kwok, H. S.; Tang, B. Z. *Thin Solid Films* **2000**, *363*, 149−151. (c) Sun, J. Z.; Chen, H. Z.; Xu, R. S.; Wang, M.; Lam, J. W. Y.; Tang, B. Z. *Chem. Commun.* **2002**, 1222−1223.

(15) (a) Chen, H. Z.; Xu, R. S.; Sun, Q. H.; Lam, J. W. Y.; Wang, M.; Tang, B. Z. *Polym. Adv. Technol.* **2000**, *11*, 442−449. (b) Tang, B. Z.; Poon, W. H.; Peng, H.; Wong, H. N. C.; Ye, X.; Monde, T. *Chin. J. Polym. Sci.* **1999**, *17*, 81−86. (c) Yao, G. J.; Dong, Y. P.; Cao, T. B.; Yang, S. M.; Lam, J. W. Y.; Tang, B. Z. *Chem. J. Chin. Univ.* **2002**, *23*, 1202−1204.

(16) (a) Tang, B. Z.; Kong, X.; Wan, X.; Feng, X.-D. *Macromolecules* **1998**, *31*, 7118. (b) Tang, B. Z.; Kong, X.; Wan, X.; Feng, X.-D. *Macromolecules* **1997**, *30*, 5620−5628. (c) Kong, X.; Tang, B. Z. *Chem. Mater.* **1998**, *10*, 3352−3363. (d) Tang, B. Z.; Kong, X.; Wan, X.; Peng, H.; Lam, W. Y.; Feng, X.; Kwok, H. S. *Macromolecules* **1998**, *31*, 2419−2432.

(17) Xu, K.; Geng, Y.; Lee, P. P. S.; Tang, B. Z. *Polym. Mater. Sci. Eng.* **2000**, *82*, 103−104.

(18) Xie, Z.; Lam, J. W. Y.; Luo, J.; Qiu, C.; Kwok, H. S.; Tang, B. Z. *Polym. Prepr.* **2001**, *42* (2), 496−497.

(19) (a) Xu, K.; Peng, H.; Lam, J. W. Y.; Poon, T. W. H.; Dong, Y.; Xu, H.; Sun, Q.; Cheuk, K. K. L.; Salhi, F.; Lee, P. P. S.; Tang, B. Z. *Macromolecules* **2000**, *33*, 6918−6924. (b) Tang, B. Z.; Xu, K.; Sun, Q.; Lee, P. P. S.; Peng, H.; Salhi, F.; Dong, Y. *ACS Symp. Ser.* **2000**, *760*, 146−164.

(20) (a) Mi, Y.; Tang, B. Z. *Polym. News* **2001**, *26*, 170−176. (b) Lam, J. W. Y.; Luo, J. D.; Peng, H.; Xie, Z. L.; Xu, K. T.; Dong, Y. P.; Cheng, L.; Qiu, C. F.; Kwok, H. S.; Tang, B. Z. *Chin. J. Polym. Sci.* **2001**, *19*, 585−590. (c) Tang, B. Z. *Chem. Res. Chin. Univ.* **2001**, *17* (3), 59.

(21) (a) Nakako, H.; Nomura, R.; Masuda, T. *Macromolecules* **2001**, *34*, 1496−1502. (b) Maeda, K.; Goto, H.; Yashima, E. *Macromolecules* **2001**, *34*, 1160−1164. (c) Nakako, H.; Mayahara, Y.; Nomura, R.; Tabata, M.; Masuda, T. *Macromolecules* **2000**, *33*, 3978−3982. (d) Nomura, R.; Fukushima, Y.; Nakako, H.; Masida, T. *J. Am. Chem. Soc.* **2000**, *122*, 8830−8836. (e) Nakako, H.; Nomura, R.; Tabata, M.; Masuda, T. *Macromolecules* **1999**, *32*, 2861−2864. (f) Tabata, M.; Inaba, Y.; Yokota, K.; Nozaki, Y. *J. Macromol. Sci., Pure Appl. Chem.* **1994**, *A31*, 465−475.

(22) For reviews, see: (a) Shirakawa, H.; Masuda, T.; Takeda, K. In *The Chemistry of Triple-Bonded Functional Groups*; Patai, S., Ed.; Wiley: New York, 1994; Suppl. C2, Chapter 17, pp 945−1016. (b) Nakano, T.; Okamoto, Y. *Chem. Rev.* **2001**, *101*, 4013−4038. (c) Yashima, E. *Anal. Sci.* **2002**, *18*, 3−6.

(23) (a) Tang, B. Z. *Polym. News* **2001**, *26*, 262−272. (b) Tang, B. Z.; Cheuk, K. K. L.; Salhi, F.; Li, B. S.; Lam, J. W. Y.; Cha, J. A. K.; Xiao, X. D. *ACS Symp. Ser.* **2001**, *812*, 133−148.

(24) Kong, X.; Lam, J. W. Y.; Tang, B. Z. *Macromolecules* **1999**, *32*, 1722−1730.

(25) (a) Imire, C. T.; Schleeh, T.; Karasz, F. E.; Attard, G. S. *Macromolecules* **1993**, *26*, 539. (b) Imire, C. T.; Karasz, F. E.; Attard, G. S. *Macromolecules* **1993**, *26*, 545.

(26) (a) *Handbook of Liquid Crystal Research*; Collings, P. J., Patel, J. S., Eds.; Oxford University Press: New York, 1997. (b) Cowie, J. M. G. *Polymers: Chemistry & Physics of Modern Materials*, 2nd ed.; Blackie: London, 1997; Chapter 16. (c) McArdle, C. B. *Side Chain Liquid Crystal Polymers*; Blackie: London, 1989.

(27) (a) Masuda, T.; Yoshimura, T.; Tamura, Y.; Higashimura, T. *Macromolecules* **1987**, *20*, 1734−1739. (b) Masuda, T.; Yamagata, M.; Higashimura, T. *Macromolecules* **1984**, *17*, 126−129.

(28) Tang, B. Z.; Kotera, N. *Macromolecules* **1989**, *22*, 4388−4390.

(29) Silverstein, R. M.; Webster, F. X. *Spectrometric Identification of Organic Compounds*, 6th ed.; Wiley: New York, 1998.

(30) Carey, F. A. *Organic Chemistry*, 3rd ed.; McGraw-Hill: New York, 1996; Chapter 10.

(31) Lambert, J. B.; Shurvell, H. F.; Lightner, D. A.; Cooks, R. G. *Organic Structural Spectroscopy*; Prentice Hall: Upper Saddle River, NJ, 1998; Chapter 3.

(32) (a) Percec, V.; Pugh, C. In *Side Chain Liquid Crystal Polymers*; McArdle, C. B., Ed.; Chapman & Hall: New York, 1989; Chapter 3, pp 30−105. (b) *Liquid Crystalline Polymer Systems*; Isayev, A. I., Kyu, T., Cheng, S. Z. D., Eds.; American Chemical Society: Washington, DC, 1996. (c) Pugh, C.; Kiste, A. L. *Prog. Polym. Sci.* **1997**, *22*, 601−691. (d) Shiota, A.; Ober, C. K. *Prog. Polym. Sci.* **1997**, *22*, 975−1000.

(33) Cowie, J. M. G. *Polymers: Chemistry and Physics of Modern Materials*, 2nd ed; Blackie: New York, 1991.

(34) This relation actually holds for all of our polyacetylene liquid crystals. For "normal" vinyl polymer liquid crystals, their T_g's are usually lower than the T_m's of their mesogens, or the glass transitions of the flexible chain segments occur before the melting transitions of the rigid mesogens.[32,33] The unusual feature of our system is the rigidity of the polyacetylene backbone, whose segmental movements are normally initiated by thermal agitations at temperatures higher than the T_m's of the mesogens. The melting of the mesogens at lower temperatures will, however, provide liquefacient "lubricants" to activate the movements of the chain segments, and the polymers thus undergo the melting and glass transitions simultaneously at the same temperatures, that is to say, T_m

= T_g. It is difficult, if not impossible, to separate these two transitions because the glass transitions are inherently associated with the melting transitions in our polyacetylene systems.

(35) Note that the DSC thermogram of the polymer was measured during the first *cooling* scan. The thermal transitions here were thus for a sample that had already been partially isomerized during the first *heating* scan.

(36) The sample was not heated to the isotropization point but not to the isomerization temperature.

(37) A polymer with a regular structure tends to undergo thermal transitions at higher temperatures: for example, a stereoregular poly(phenylacetylene) shows a higher melting temperature than does a random one.[16b]

(38) *Liquid Crystalline Order in Polymers*; Blumstein, A., Hsu, E. C., Eds.; Academic Press: New York, 1978.

(39) Liu, Z.; Zhu, L.; Zhou, W.; Cheng, S. Z. D.; Percec, V.; Ungar, G. *Chem. Mater.* **2002**, *14*, 2384−2392 and references therein.

(40) (a) The acetylene polymerizations through the Mo-catalyzed metathesis routes generally yield stereoirregular polymers. Like **1**-Mo, polymers **2**(-Mo) and **3**(-Mo) also possess stereoirregular structures, as suggested by the broad peaks of their ^{1}H NMR spectra (not shown). (b) Molecular weights of substituted polyacetylenes had little effects on their absorption spectra: Dong, Y.; Lam, J. W. Y.; Cha, J. A. K.; Tang, B. Z. *Polym. Mater. Sci. Eng.* **2001**, *84*, 539−540.

(41) The conjugation of the repeat unit may be similar to that of *trans*-stilbene, whose λ_{max} and ϵ_{max} are 250 nm and 25 000 mol^{-1} L cm^{-1}, respectively. (a) Silverstein, R. M.; Bassler, G. C.; Morrill, T. C. *Spectrometric Identification of Organic Compounds*, 5th ed.; Wiley: New Youk, 1991; Chapter 7. (b) Pretsch, E.; Buhlmann, P.; Affolter, C. *Structure Determination of Organic Compounds: Table of Spectral Data*, 3rd ed.; Springer: Hong Kong, 2000; Chapter 8.

(42) (a) Luo, J. D.; Xie, Z. L.; Lam, J. W. Y.; Cheng, L.; Chen, H. Y.; Qiu, C. F.; Kwok, H. S.; Zhan, X. W.; Liu, Y. Q.; Zhu, D. B.; Tang, B. Z. *Chem. Commun.* **2001**, 1740−1741. (b) Tang, B. Z.; Zhan, X.; Yu, G.; Lee, P. P. S.; Liu, Y. Q.; Zhu, D. B. *J. Mater. Chem.* **2001**, *11*, 2874−2978. (c) Freemantle, M. *Chem. Eng. News* **2001**, *79* (1), 29. (d) Chen, H. Y.; Lam, J. W. Y.; Luo, J. D.; Ho, Y. L.; Tang, B. Z.; Zhu, D. B.; Wong, M.; Kwok, H. S. *Appl. Phys. Lett.* **2002**, *81*, 574−576.

(43) (a) Kim, J.; Swager, T. M. *Nature (London)* **2001**, *411*, 1030−1034. (b) de Boer, B.; Stalmach, U.; van Hutten, P. F.; Melzer, C.; Krasnikov, V. V.; Hadziioannou, G. *Polymer* **2001**, *42*, 9097−9109. (c) Wang, Y. Z.; Gebler, D. D.; Fu, D. K.; Swager, T. M.; MacDiarmid, A. G.; Epstein, A. J. *Synth. Met.* **1997**, *85*, 1179−1182.

(44) (a) Hidayat, R.; Tatsuhara, S.; Kim, D. W.; Ozaki, M.; Yoshino, K.; Teraguchi, M.; Masuda, T. *Phys. Rev. B* **2000**, *61*, 10167. (b) Frolov, S. V.; Fujii, A.; Chinn, D.; Hirohata, M.; Hidayat, R.; Taraguchi, M.; Masuda, T.; Yoshino, K.; Vardeny, Z. V. *Adv. Mater.* **1998**, *10*, 869.

(45) (a) Sun, R. G.; Zheng, Q. B.; Zhang, X. M.; Masuda, T.; Kobayashi, T. *Jpn. J. Appl. Phys.* **1999**, *38*, 2017. (b) Sun, R. G.; Masuda, T.; Kobayashi, T. *Synth. Met.* **1997**, *91*, 301.

(46) (a) Friend, R. H.; Gymer, R. W.; Holmes, A. B.; Burroughes, J. H.; Marks, R. N.; Taliani, C.; Bradley, D. D. C.; Dos Santos, D. A.; Bredas, J. L.; Logdlund, M.; Salaneck, W. R. *Nature (London)* **1999**, *397*, 121−128. (b) Li, X.-C.; Moratti, S. C. In *Photonic Polymer Systems: Fundamentals, Methods, and Applications*; Wise, D. L., Wnek, G. E., Trantolo, D. J., Cooper, T. M., Gresser, J. D., Eds.; Marcel Dekker: Hong Kong, 1998; Chapter 10, pp 335−371. (c) Heeger, A. J.; Diaz-Garcia, M. A. *Curr. Opin. Solid State Mater. Sci.* **1998**, *3*, 16−22.

(47) Son, S.; Dodabalapur, A.; Lovinger, A. J.; Galvin, M. E. *Science* **1995**, *269*, 376−378.

(48) (a) Xie, Z. L.; Lam, J. W. Y.; Chen, J. W.; Dong, Y. P.; Qiu, C. F.; Wong, M.; Kwok, H. S.; Tang, B. Z. *Polym. Prepr.* **2002**, *43* (1), 411−412. (b) Xie, Z. L.; Lam, J. W. Y.; Chen, J. W.; Dong, Y. P.; Qiu, C. F.; Wong, M.; Kwok, H. S.; Tang, B. Z. *Polym. Prepr.* **2002**, *43* (1), 551−552. (c) Xie, Z. L.; Lam, J. W. Y.; Chen, J. W.; Dong, Y. P.; Qiu, C. F.; Kwok, H. S.; Tang, B. Z. *Polym. Mater. Sci. Eng.* **2002**, *86*, 185−186. (d) Lam, J. W. Y.; Xie, Z. L.; Chen, J. W.; Dong, Y. P.; Qiu, C. F.; Kwok, H. S.; Tang, B. Z. *Polym. Mater. Sci. Eng.* **2002**, *86*, 231−232.

(49) (a) Xie, Z. L.; Lam, J. W. Y.; Qiu, C. F.; Luo, J. D.; Tang, B. Z.; Kwok, H. S. *Asia Display/IDW* **2001**, 1451−1453. (b) Xie, Z.; Lam, J. W. Y.; Luo, J.; Qiu, C.; Kwok, H. S.; Tang, B. Z. *Polym. Prepr.* **2001**, *42* (2), 496−497. (c) Dong, Y.; Lam, J. W. Y.; Lee, P. P. S.; Tang, B. Z. *Polym. Mater. Sci. Eng.* **2001**, *84*, 639−640. (d) Dong, Y. P.; Lam, J. W. Y.; Tang, B. Z. *Polym. Mater. Sci. Eng.* **2001**, *84*, 616−617. (e) Dong, Y. P.; Lam, J. W. Y.; Cha, J. A. K.; Tang, B. Z. *Polym. Mater. Sci. Eng.* **2001**, *84*, 539−540.

(50) Zhou, Q. F.; Wan, X. H.; Zhang, D.; Feng, X. D. *ACS Symp. Ser.* **1996**, *632*, 344−357.

(51) E.g.: (a) Schenning, A. P. H. J.; Fransen, M.; Meijer, E. W. *Macromol. Rapid Commun.* **2002**, *23*, 266−270. (b) Ting, C. H.; Chen, J. T.; Hsu, C. S. *Macromolecules* **2002**, *35*, 1180−1189. (c) Kuroda, H.; Goto, H.; Akagi, K.; Kawaguchi, A. *Macromolecules* **2002**, *35*, 1307−1313. (d) Stagnaro, P.; Cavazza, B.; Trefiletti, V.; Costa, G.; Gallot, B.; Valenti, B. *Macromol. Chem. Phys.* **2001**, *202*, 2065−2073. (e) Koltzenburg, S.; Wolff. D.; Stelzer, F.; Springer, J.; Nuyken, O. *Macromolecules* **1998**, *31*, 9166−9173.

(52) Tang, B. Z.; Poon, W. H.; Leung, S. M.; Leung, W. H.; Peng, H. *Macromolecules* **1997**, *30*, 2209−2212.

MA021011A